

Conceptual design and scaled experimental validation of an actively damped carbon tie rods support system for the stabilization of future particle collider superstructures

C. Collette, D. Tshilumba, L. Fueyo-Rosa, and I. Romanescu

Citation: *Rev. Sci. Instrum.* **84**, 023302 (2013); doi: 10.1063/1.4789783

View online: <http://dx.doi.org/10.1063/1.4789783>

View Table of Contents: <http://rsi.aip.org/resource/1/RSINAK/v84/i2>

Published by the [American Institute of Physics](#).

Related Articles

Record high-average current from a high-brightness photoinjector
Appl. Phys. Lett. **102**, 034105 (2013)

Improved charge breeding efficiency of light ions with an electron cyclotron resonance ion source
Rev. Sci. Instrum. **83**, 113303 (2012)

Ion acceleration from thin foil and extended plasma targets by slow electromagnetic wave and related ion-ion beam instability
Phys. Plasmas **19**, 103105 (2012)

Quasi-monoenergetic electron beams production in a sharp density transition
Appl. Phys. Lett. **101**, 111106 (2012)

A polyvalent harmonic coil testing method for small-aperture magnets
Rev. Sci. Instrum. **83**, 085116 (2012)

Additional information on *Rev. Sci. Instrum.*

Journal Homepage: <http://rsi.aip.org>

Journal Information: http://rsi.aip.org/about/about_the_journal

Top downloads: http://rsi.aip.org/features/most_downloaded

Information for Authors: <http://rsi.aip.org/authors>

ADVERTISEMENT

AEROTECH®

MPS-SL Mechanical-Bearing Ball-Screw Linear Stages

- Compact 50-75 mm width with travel up to 100 mm
- Precision ground ball-screw or lead-screw drive
- DC servo or stepper motor
- Crossed-roller bearings
- High resolution (0.1 μ m), repeatability ($\pm 0.75 \mu$ m) and accuracy ($\pm 1.0 \mu$ m)
- High vacuum capable
- Compact multi-axis configurations

Conceptual design and scaled experimental validation of an actively damped carbon tie rods support system for the stabilization of future particle collider superstructures

C. Collette,^{1,a)} D. Tshilumba,¹ L. Fueyo-Rosa,¹ and I. Romanescu²

¹Active Structures Laboratory, Department of Mechanical Engineering and Robotics, Université Libre de Bruxelles, 50, av. F.D. Roosevelt, 1050 Brussels, Belgium

²Department of Machine-Tools, Technical University Gheorghe Asachi of Iasi, 67, Dimitrie Mangeron Bd., 700050 Iasi, Romania

(Received 31 October 2012; accepted 15 January 2013; published online 4 February 2013)

This paper presents a simple solution to increase the stability of the large superstructures supporting the final electromagnets of future linear particle collider. It consists of *active carbon fiber tie rods*, fixed at one end on the structure and at the other end to the detector through active tendons. In the first part of the paper, the solution has been tested on a finite element model of one half of the CLIC_ILD final focus structure. With a reasonable design, it is shown numerically that the compliance can be decreased by at least a factor 4, i.e., that the structure is 4 times more robust to technical noise at low frequency. Two additional features of the active rods are that they can also actively damp the structural resonances and realign the superstructures. The second part of the paper presents a successful experimental validation of the concept, applied to a scaled test bench, especially designed to contain the same modal characteristics as the full scale superstructure. © 2013 American Institute of Physics. [<http://dx.doi.org/10.1063/1.4789783>]

I. INTRODUCTION

In order to continue the exploration of high energy physics, several projects of linear particle colliders have been proposed, like the compact linear collider (CLIC),^{1,2} under study at CERN, or the international linear collider (ILC),³ under study at SLAC. In these future machines, the *luminosity* (i.e., density of the particle collisions) will be extremely high, which has two implications. First, the instrument is extremely sensitive to ground vibrations and environmental disturbances.^{4–13} Second, it imposes to place the last electromagnets (called QD0) close to each other. Unfortunately, as the size of the detector cannot be downscaled, the QD0 should be mounted inside the detector. Several designs have been proposed in the literature.¹⁴ Currently, two detector concepts are still under study for ILC: the SiD¹⁵ and the ILD,¹⁶ which have been adapted for CLIC under the names CLIC_SiD and CLIC_ILD.^{17,18} In the first one, the quadrupoles are supported inside the detector. In the second one, the quadrupoles are supported inside big tubes, cantilevered to the tunnel walls. These tubes are the superstructures that we propose to stabilize.

In Ref. 3, the idea to use tie rods to hang the tube which supports QD0 was first introduced for the ILD detector. In that case, only two vertical tie rods have been proposed to compensate the weight of the structure. On the other hand, in Ref. 19, it has been shown on a simplified model that the introduction of active stiffeners to the superstructure, like active cables or active tie rods, can fulfill several important tasks. First, the additional stiffness enables to increase the robustness of the end of the tube to the technical noise, by reduc-

ing the tube compliance. Second, the resonances of the tube can be damped actively using the active tendons mounted at the outer end of each stiffener. Third, they can also be used to realign the two structures, instead of the alignment stage currently foreseen at the frame of the tube. In this paper, we propose to use a network of active tie rods, which will both hang the structure, but also fulfill the three tasks mentioned here above. The solution proposed in this paper is applied on the CLIC_ILD detector. Nevertheless, it can be easily applied to the SiD type.

Section II presents the model of the structure supporting one QD0 quadrupole, along with a conceptual design of the stabilization system. Section III presents the scaled test bench developed to validate the concept of active tie rods and shows the experimental results. Section IV draws the conclusions.

II. SUPERSTRUCTURE STABILIZATION

A. Finite element model

The model of the superstructure supporting the last quadrupole (QD0) of the CLIC_ILD detector is shown in Fig. 1(a). It consists of a large tube, cantilevered on the tunnel wall, inside which QD0 is mounted.

Compared to the original drawings, the analysis has been performed using the following simplifications: (1) All parts are made of stainless steel ($E = 200$ Gpa, $\rho = 7600$ kg/m³); (2) All parts in contacts have been rigidly glued; (3) The external tube has been modeled with beam elements; (4) The pre-isolator²⁰ has been rigidly fixed on the ground; (5) the cam system foreseen to realign the tube²¹ has been removed. Table I summarizes the main characteristics of the elements of the superstructure, along with the hypothesis used in the

^{a)}Author to whom correspondence should be addressed. Electronic mail: ccollett@ulb.ac.be.

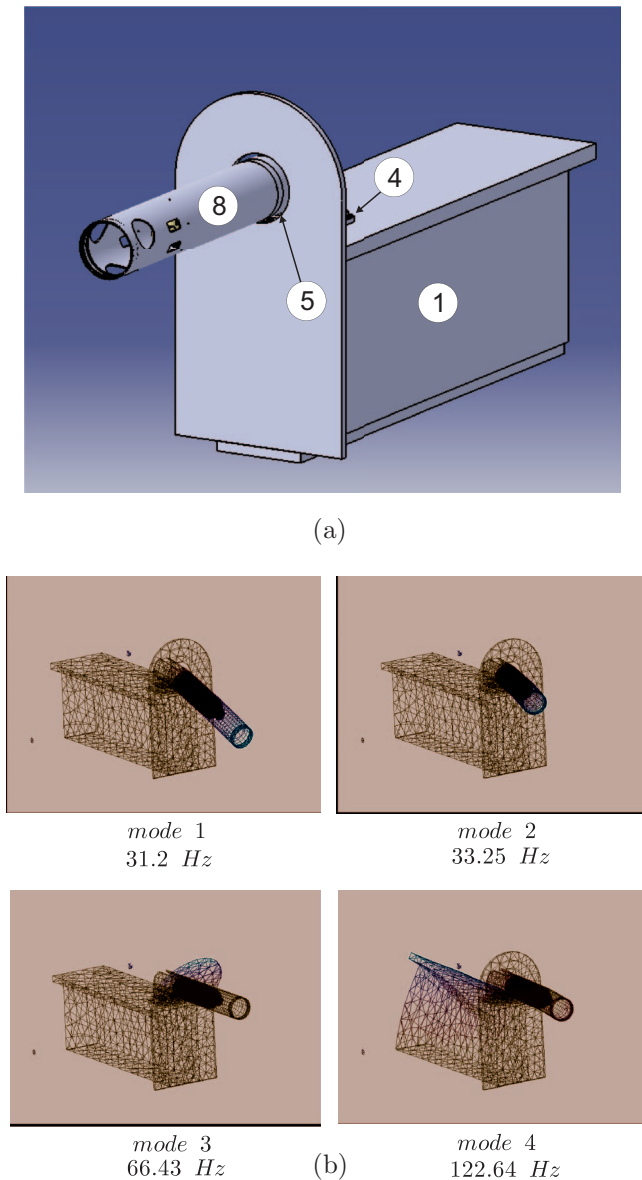


FIG. 1. Superstructure supporting one QD0 in the CLIC_ILD detector: (a) drawing; (b) first four resonances.

finite element model. Those which are visible in Fig. 1 are indicated by their corresponding number.

Figure 1(b) shows the eigen modes and frequencies obtained under these assumptions. The first bending mode of the tube is about 30 Hz, and the higher modes are above 60 Hz. In order to extract the compliance from the finite element model, we have used a sub-structuring method to obtain the dynamic equations of the system, keeping only the first twenty resonance modes. The dynamics equation reads

$$\mathbf{M}\mathbf{s}^2\mathbf{x} + \mathbf{C}\mathbf{s}\mathbf{x} + \mathbf{K}\mathbf{x} = \mathbf{F}, \quad (1)$$

where \mathbf{M} is the mass matrix, \mathbf{C} is the damping matrix, \mathbf{K} is the stiffness matrix, \mathbf{x} is the vector of structural degrees of freedom (d.o.f.), and \mathbf{F} is the vector of disturbing forces.

From Eq. (1), one can calculate the compliance of the structure, i.e., the ratio between \mathbf{x} and \mathbf{F} . For example, Fig. 2 shows the compliance of the free end of the superstructure in the vertical direction.

TABLE I. Characteristics of the main elements of the CLIC_ILD superstructure, along with the hypothesis used in the finite element model.

Part	Dimensions [mm]	Volume [m ³]	Element type
1. Pre-isolator	$L = 1610^3$ $l = 2.510^3$ $h = 3.2510^3$	41	Volume
2. Quadrupole	$L = 2.710^3$ $l = 300$ $h = 423.6$	188.29710^{-3}	Volume
3. Quadrupole Support	$L = 2.1310^3$ $l = 266.36$ $h = 64.26$	44.7710^{-3}	Volume
4. Pre-alignment support system	$L = 1.310^3$ $l = 1.110^3$ $h = 78.997$	121.6610^{-3}	Volume
5. Tube fixation part	$r_{int} = 418$ $r_{ext} = 475$ $L = 1.510^3$	295.3110^{-3}	Volume
6. Reinforcement tube	$r_{int} = 347.825$ $r_{ext} = 448.275$	243.2310^{-3}	Volume
7. Reinforcement Ring	$r_{int} = 427.5$ $r_{ext} = 475$	29.9410^{-3}	Volume
8. Tube	$r_{int} = 455$ $r_{ext} = 475$ $L = 4.3810^3$	255.9310^{-3}	Beam

B. Tie rods design

As mentioned in the introduction, the objectives of the tie rods are to stiffen the superstructure, damp it actively, and provide it with some positioning capability. Each rod is connected at one end to the superstructure and at the other end to the detector. For simplicity, the tie rods are considered as mass-less springs. As the rods are located inside the detector, they must be as non-invasive as possible. This means that we should mount only a small number of thin rods. In order to determine the suitable number of rods and their dimension, one must first determine the equivalent static stiffness k_{eq} of the cantilevered structure. In the vertical direction, it has been determined by applying a static force at the free end of the tube of $F = 10$ kN. It induced a displacement of $\Delta x = 0.2241$ mm, from which we deduced that $k_{eq} = 4.4610^7$ N/m. Because of

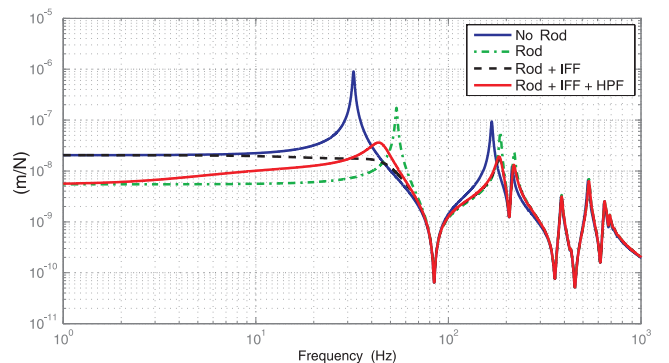


FIG. 2. Compliance of the free end of the tube superstructure in the vertical direction.

TABLE II. Number of tie rods and corresponding dimensions to obtain a stiffness of $k_r^t = 13.3810^7$ N/m.

n [-]	A_r [mm 2]	d_r [mm]
1	2467.9	56.1
2	1234	39.64
3	822.64	32.364
4	616.975	28.03

the symmetry of the structure, the same value is obtained for the lateral direction. With an array of tie rods, the new static stiffness will be $k_{eq} + k_r^t$, where k_r^t is the total stiffness in one direction. As an example, consider that we want to increase the first resonance by a factor two, i.e., decrease the compliance by a factor 4 in both the vertical and the lateral direction. Then, k_r^t satisfies the equation

$$k_{eq} + k_r^t = 4k_{eq}, \quad (2)$$

which means that the additional stiffness in both the vertical and the lateral direction should be

$$k_r^t = 13.3810^7 \text{ N/m}. \quad (3)$$

For a network of n identical rods in the same direction, we have

$$k_r^t = n \frac{E_r A_r}{L_r} = \frac{E_r A_r^t}{L_r}, \quad (4)$$

where E_r is the Young modulus of the rods, A_r the area of a rod cross section, and L_r its length. A_r^t the area of the sum of the cross sections of the n rods. The material chosen for the rods is carbon ($E_r = 180$ Gpa) and the length is fixed by the size of the detector ($L_r = 3.32$ m). Thus, from Eq. (4), we get $A_r^t = 2467.9$ mm 2 . Table II gives the corresponding number of rods necessary to fulfil Eq. (3), along with the rod circular cross section area A_r and diameter d_r .

From Table II, we find that the compliance can be decreased by a factor four in both the vertical and lateral direction, using two rods with a diameter $d_r = 39.64$ mm in each direction. The embodiment is shown in Fig. 3(a) and 3(b) shows the first four resonance modes. Indeed, the resonance frequencies of the first two modes have been increased by a factor two (see Fig. 1(b) for comparison).

Including the rods, Eq. (1) becomes

$$\mathbf{M} s^2 \mathbf{x} + \mathbf{C} s \mathbf{x} + \mathbf{K} \mathbf{x} = \mathbf{L} \mathbf{T} + \mathbf{F}, \quad (5)$$

where \mathbf{T} is a vector containing the tensions in the tie rods and \mathbf{L} is the influence matrix, to express the tensions in the structural degrees of freedom. The tension T_i in the rod i results from the extension q_i of the rod i such as

$$T_i = k_r q_i \quad (6)$$

and the extensions are also connected to the d.o.f. of the structure by the influence matrix

$$\mathbf{q} = \mathbf{L}^T \mathbf{x}. \quad (7)$$

The new compliance of the free end of the superstructure reinforced by the tie rods is also shown in Fig. 2, which clearly

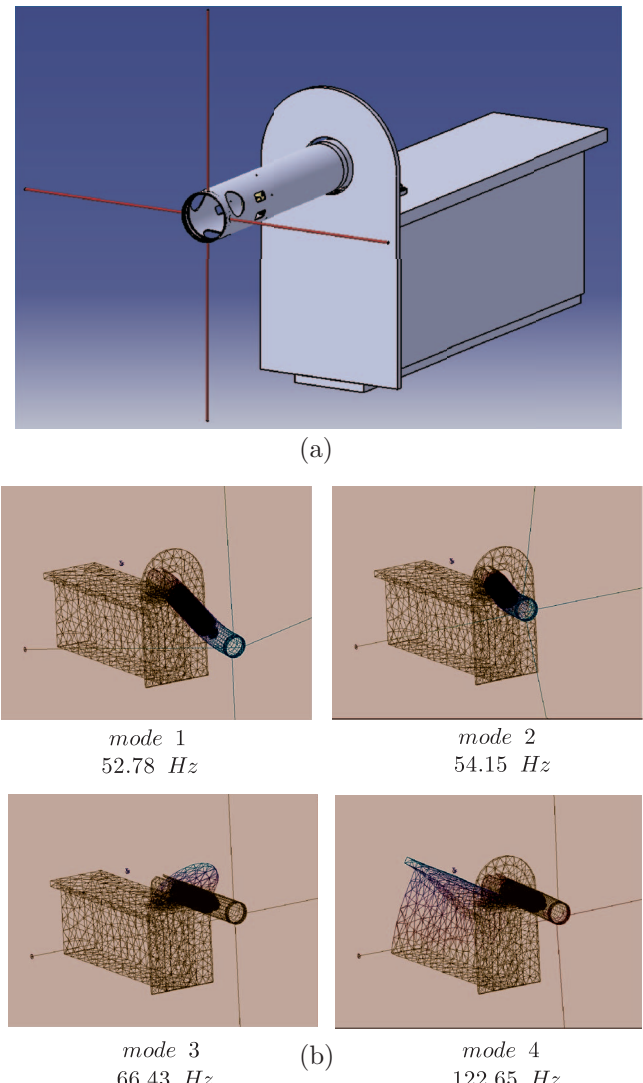


FIG. 3. Superstructure supporting one QD0 in the CLIC-ILD detector, reinforced with a network of four carbon tie rods: (a) drawing; (b) first four resonances.

shows that it has been reduced by a factor four in the low frequency range.

As mentioned in the introduction, we also propose to fix the rods on the detector through active tendons, to increase actively the structural damping and provide it positioning capabilities. This is discussed in Sec. II C.

C. Structural control with active tendons

Now consider that each tie rod is connected to the detector through an active tendon, consisting of a force sensor in series with a piezoelectric actuator. Thus, the tension T_i in the rod i results from the relative displacement of the ends of the rod q_i minus the elongation δ_i of the displacement actuator i , such as

$$T_i = k_r(q_i - \delta_i). \quad (8)$$

Next, let us also consider decentralized Single Input Single Output (SISO) controllers in each active tendon, i.e., that

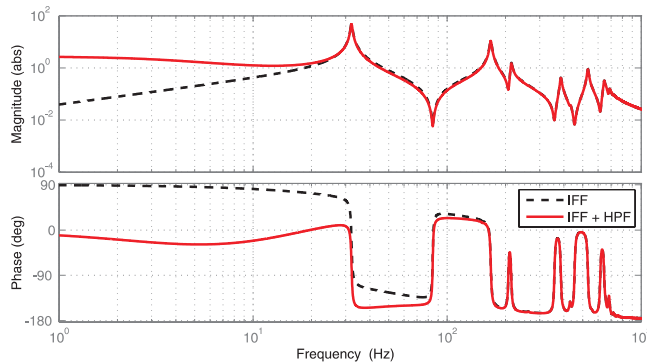


FIG. 4. Open loop transfer function between the force exerted by a vertical tendon on the superstructure and its vertical displacement at the same location for two controllers: IFF and IFF filtered.

each actuator is controlled using the signal from the force sensor of the same tendon. Mathematically,

$$\delta_i = g H_r(s) T_i / k_r, \quad (9)$$

where $H_r(s)$ is the control filter and g is the gain. It follows that Eq. (5) becomes

$$\mathbf{M} s^2 \mathbf{x} + \mathbf{C} s \mathbf{x} + \left[\mathbf{K} + \frac{k_r}{1 + g H_r(s)} \mathbf{L} \mathbf{L}^T \right] \mathbf{x} = \mathbf{F}. \quad (10)$$

From Eq. (10) one sees that the new stiffness matrix is

$$\left[\mathbf{K} + \frac{k_r}{1 + g H_r(s)} \mathbf{L} \mathbf{L}^T \right].$$

In order to add some damping in the structure, let us use an integral force feedback (IFF) strategy^{22,23}

$$H_r(s) = \frac{1}{s}. \quad (11)$$

In this case, Eq. (10) becomes

$$\mathbf{M} s^2 \mathbf{x} + \mathbf{C} s \mathbf{x} + \left[\mathbf{K} + k_r \frac{s}{s + g} \mathbf{L} \mathbf{L}^T \right] \mathbf{x} = \mathbf{F}. \quad (12)$$

It is shown in Ref. 23 and 24 that the maximum damping of mode i , ξ_i^{\max} is given by

$$\xi_i^{\max} = \frac{\Omega_i - \omega_i}{2\omega_i} \quad (13)$$

and it is obtained for a gain g_i of

$$g_i = \Omega_i \sqrt{\Omega_i / \omega_i}, \quad (14)$$

which is different for each mode. At low frequency, the response of the structure is, to a large extent, dominated by the first resonance, for which the optimal value of the gain is $g_1 = 337 * \sqrt{337/200} = 437.45$ and the damping of the first mode is $\xi_1^{\max} = 0.35$.

Figures 4 and 2, respectively, show the open loop transfer function between the forces exerted by the tendons and structural displacement at the locations where the tie rods are attached and the compliance obtained with the optimal gain.

A drawback of this controller is that the structural damping is obtained at the cost of a degradation of the compliance at low frequency. Indeed, taking $s \rightarrow 0$ in Eq. (12) clearly shows that, at low frequency, the tie rods do not participate in

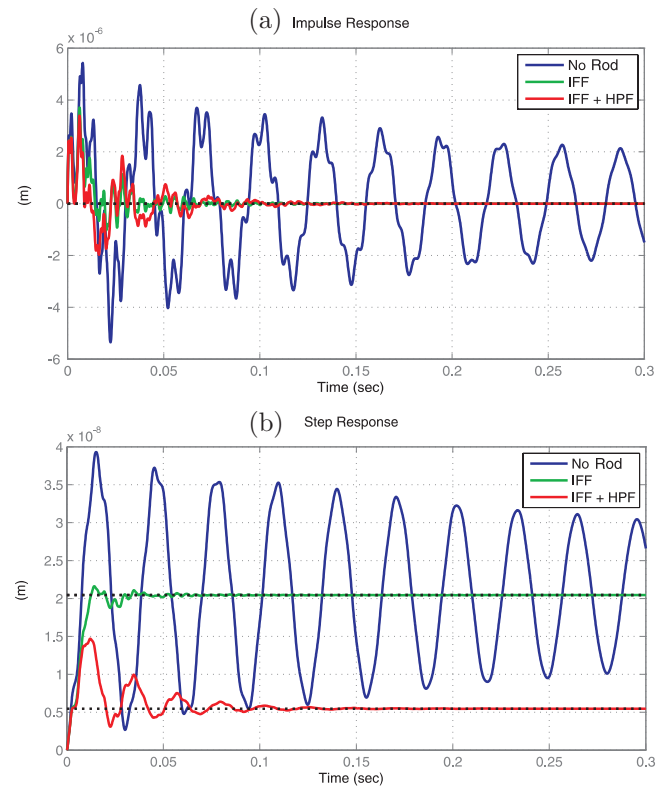


FIG. 5. Time response of the free end of the superstructure in the vertical direction, excited at the same location: (a) impulse response; (b) step response.

the stiffness matrix anymore. To improve the low frequency behavior, one can add a high pass filter (HPF) to the controller and Eq. (11) becomes²⁵

$$H_r(s) = \frac{s}{(s + a)^2}, \quad (15)$$

where a is a design parameter limiting the effect of the IFF at low frequency. If $s > a$ the controller is the same as Eq. (11). Again, Figs. 4 and 2, respectively, show the open loop transfer function and the compliance for an intermediate value of $a = 0.6\omega_1$, and the same value of the gain as before. The filter allows to recover a low compliance at low frequency, but at the cost of a slightly reduced damping. This is a fundamental tradeoff of the controller.

In order to illustrate the performances of the two controllers in the time domain, Figs. 5(a) and 5(b) show the impulse and step response of the free end of the superstructure, excited at the same degree of freedom, without and with tie rods.

The impulse response shows that the active tie rods allow a rapid stabilization of the structure, even faster with non filtered IFF than with the filtered one (because of the higher level of damping). On the other hand, the step response illustrates that the filtered IFF is more robust to low frequency external disturbances.

In order to validate experimentally the concepts proposed in this section, a test bench has been developed, representing the superstructure at roughly a quarter scale. It is described in Sec. III.

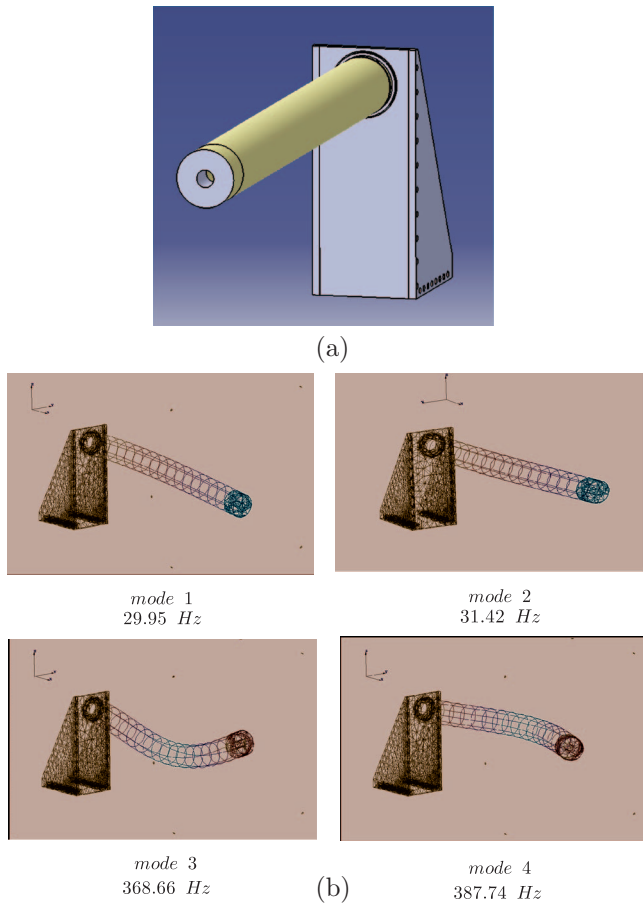


FIG. 6. Scaled test bench: (a) drawing; (b) first four eigen modes.

III. SCALED TEST BENCH

A. Modeling and simulations

Figures 6 and 7 show the drawing of the test bench without and with rods, along with the first four eigen modes for both configurations. Compared to the full scale superstructure, the ratio between the length of the tube and its diameter has been modified to keep the first resonance frequency in the same range of values. The set-up is made of aluminium ($E_{al} = 70$ GPa, $\rho_{al} = 2710$ kg/m³). The values of k_{eq} and k_c^{tot} have been determined by following exactly the same procedure as in Sec. II B. For convenience, it has been chosen to reinforce the structure with carbon fibre cable *dyneema* ($E \sim 70$ GPa). In tension, cables play exactly the same role as rods. The length of the cables has been fixed at $L_c = 20$ cm. With a diameter $d_c = 0.767$ mm the theoretical equivalent stiffness is $k_c = 1.6210^5$ N/m.

B. Structural control

The procedure to assess the performances for the scaled test bench is similar to the procedure developed for the full scale superstructure in Sec. II C. The compliance at the free end of the scaled tube is shown in Fig. 8.

Compared to the full scale superstructure, the response is more dominated by the first resonance. Here again, the two controllers are tested: IFF and IFF filtered with a HPF.

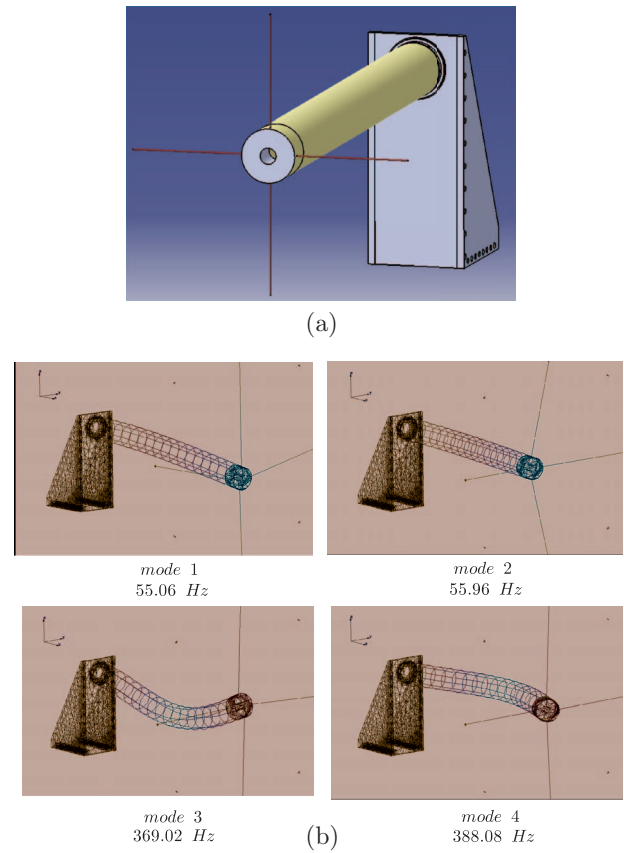


FIG. 7. Scaled test bench with carbon rods: (a) drawing; (b) first four eigen modes.

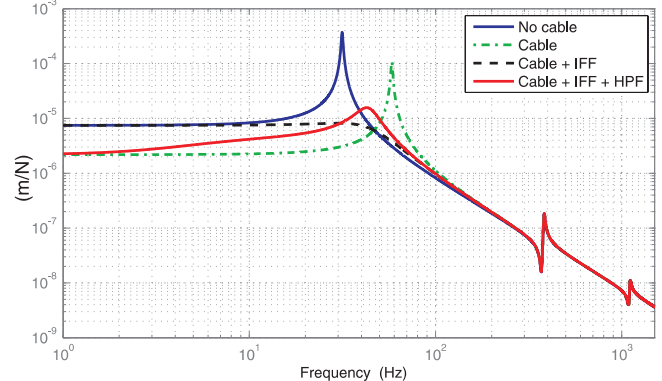


FIG. 8. Compliance of the scaled test bench at the free end of the tube in the vertical direction.

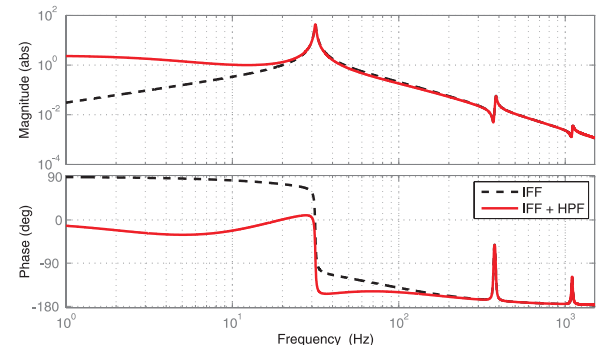


FIG. 9. Open loop transfer function between the force exerted by a vertical tendon on the scaled tube and its vertical displacement at the same location for two controllers: IFF and IFF filtered.

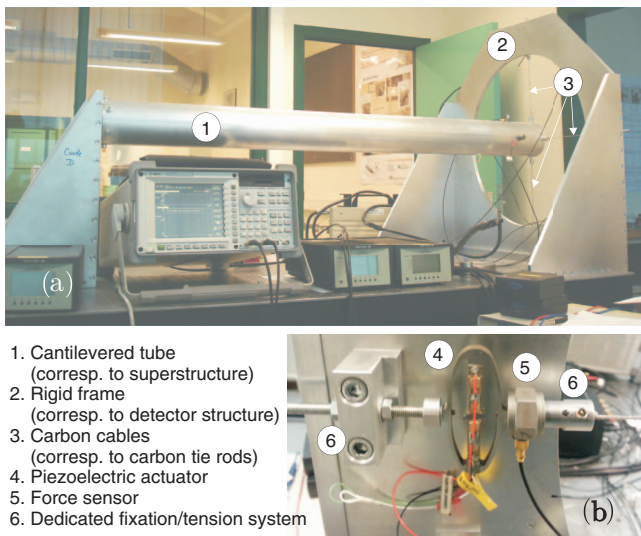


FIG. 10. (a) Picture of the experimental set-up. (b) Active tendon.

Figures 8 and 9, respectively, show the compliance at the end of the tube and the open loop transfer function.

The optimal gain chosen to maximize the damping of the first mode is $g = 365 * \sqrt{365/198}$ and the corresponding damping is $\xi_1^{\max} = 0.42$.

In the time domain, the performances are also found to be very similar to those obtained for the full scale model (Fig. 5).

C. Experimental results

Figure 10(a) shows a picture of the experimental set-up and Fig. 10(b) shows a zoom on an active tendon. The detector has been represented by a rigid frame. The compliance has been measured in the vertical and lateral direction by exciting the structure with an instrumented impact hammer and measuring the displacements at the same locations. It is shown in Fig. 11 for the vertical direction.

A characteristic of the cables is that they have a non-linear phenomenological law between the tension and the extension, i.e., that their stiffness is increasing as a function of the static tension. In the experiment, the tension has been

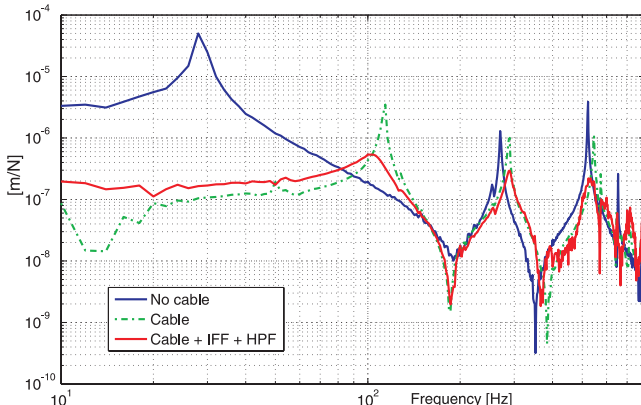
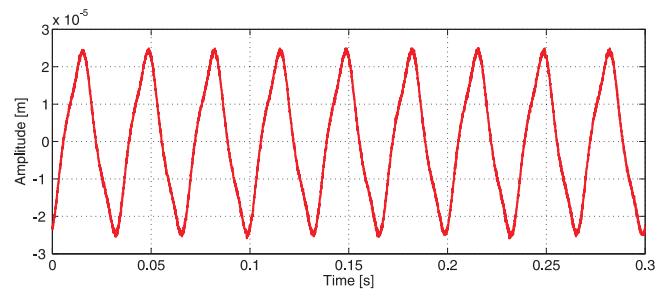


FIG. 11. Measured compliance of the end of the tube in the vertical direction.

FIG. 12. Time history of the vertical displacement of the free end of the tube, excited by a sinusoidal extension of the actuators, with an amplitude of $30 \mu\text{m}$ and a frequency of 30 Hz .

gradually increased until the first structural resonance has been multiplied by a factor three (Fig. 11). One sees that the compliance has been divided by a factor 30 at low frequency and, around 30 Hz , by more than two orders of magnitude. Theoretically, a higher reduction of the compliance could be obtained by an additional tension in the cables. However, too high a value of the tension becomes risky for the force sensors. The filtered integral force feedback has also been implemented in four decentralized loops, as described in Sec. II C. One sees that the controller adds damping on all the modes.

Finally, in order to verify the capability of the actuators to move the free end of the tube, out of phase sinusoidal signals have been injected in the two vertical actuators, with an amplitude of $30 \mu\text{m}$ and a frequency of 30 Hz . An example of the resulting time history of the vertical displacement of the tube is shown in Fig. 12. It has been measured with a laser Doppler vibrometer. One sees that the tube follows the motion imposed by the actuators, even though the amplitude is slightly smaller than $30 \mu\text{m}$, because the motion is partly compensated by structural deformations.

IV. CONCLUSIONS

The high luminosity constraint imposed to future linear particle colliders implies that the last electromagnets (quadrupoles QD0) are placed inside the detector. One possibility is to mount them on large superstructures cantilevered to the tunnel wall, which unfortunately do not constitute very stable supports. In this paper, it has been proposed to reinforce the superstructure with a network of active tie rods. Using a simple and realistic design, it has been shown numerically that the compliance of the superstructure can be reduced by a factor 4, with only four tie rods. In addition to stiffening, it has been shown that the structural damping can be significantly increased with the active tendons. A third property of the active tendons is that they can also be used to realign the superstructure. These results have been confirmed experimentally on a scaled test bench. It has been shown that a network of four cables decreased the compliance of the test bench by a factor 30. The capability of the active tendons to increase the structural damping and to reposition the structure is also confirmed experimentally, and found to comply with the theoretical predictions.

ACKNOWLEDGMENTS

The research leading to these results has been funded by the Brain Back to Brussels program from Brussels Capital Region. The authors also gratefully acknowledge Bastien Legrand for his help in the calculations, Arnaud Mewissen for inspiring discussions on the mechanical design, and Julien Amar for his help to conduct the experiments.

¹J. P. Delahaye, "Towards CLIC feasibility," in *Proceedings of the IEEE International Particle Accelerator Conference IPAC10, Kyoto, Japan, 2010*, pp. 23–25.

²See <http://clic-stability.web.cern.ch/clic-stability/> for information about the CLIC, and the studies on the vibration control of the CLIC electromagnets.

³ILC reference design report, Technical Report ILC-Report-2007-01, 2007.

⁴R. W. Assmann, J. B. Jeanneret, A. Verdier, L. Vos, E. Wildner, F. Zimmermann, R. Brinkmann, C. Montag, I. Reyzi, N. Walker, C. E. Adolphsen, J. Frisch, N. Phinney, T. O. Raubenheimer, A. Seryi, and P. G. Tenenbaum, "Stability considerations for final focus systems of future linear colliders," in *Proceedings of the 7th European Particle Accelerator Conference, Vienna, Austria, 26–30 June 2000*.

⁵A. Seryi, M. Breidenbach, and J. Frisch, "Ground motion studies and modeling for the interaction region of a linear collider," in *Proceedings of the 20th International Linear Accelerator Conference, Monterey, CA, USA, 21–25 August 2000*.

⁶M. Aleksa, R. W. Assmann, W. Coosemans, G. Guignard, N. Leros, M. Mayoud, S. Redaelli, F. Ruggiero, S. Russenschuck, D. Schulte, I. H. Wilson, and F. Zimmermann, "The CLIC study of magnet stability and time-dependent luminosity performance," in *Proceedings of the 19th IEEE Particle Accelerator Conference, Chicago, IL, USA, 18–22 June 2001*.

⁷S. Redaelli, "Stabilization of nanometre-size particle beams in the final focus system of the compact linear collider (CLIC)," Ph.D. dissertation (EPFL, Lausanne, 2003).

⁸L. Hendrickson, J. Frisch, T. Himel, A. Raubenheimer, A. Seryi, M. Woodley, and G. White, "Simulations of IP feedback and stabilization in the NLC," in *Proceedings of the EPAC 04, Lucerne, Switzerland, 2004*.

⁹J. Frisch, A. Chang, V. Decker, E. Doyle, L. Eriksson, L. Hendrickson, T. Himel, T. Markiewicz, R. Partidge, and A. Seryi, "Vibration stabilization of a mechanical model of a X-band linear collider final focal magnet," in *Proceedings of the 22nd International Linear Collider Conference, 16–18 August, 2004, Germany*.

¹⁰Andrei Seryi, Linda Hendrickson, and Glen White, "Issues of stability and ground motion in ILC," Technical Report SLAC-PUB-11661 (SLAC, Stanford, CA, 2006).

¹¹B. Parker, A. Mikhailichenko, K. Buesser, J. Hauptman, T. Tauchi, P. Burrows, T. Markiewicz, M. Oriunno, and A. Seryi, "Functional requirements on the design of the detectors and the interaction region of an e+e-linear collider with a push-pull arrangement of detectors," Technical Report EuCARD-CON-2009-026, 2009.

¹²C. Collette, K. Artoos, A. Kuzmin, S. Janssens, M. Sylte, M. Guinchard, and C. Hauviller, *Nucl. Instrum. Methods Phys. Res. A* **621**(1–3), 71–78 (2010).

¹³C. Collette, S. Janssens, K. Artoos, A. Kuzmin, P. Fernandez-Carmona, M. Guinchard, R. Leupe, and C. Hauviller, *Nucl. Instrum. Methods Phys. Res. A* **643**(1), 95–101 (2011).

¹⁴A. Seryi, *Nucl. Instrum. Methods Phys. Res. A* **623**, 23–28 (2010).

¹⁵H. Aihara *et al.*, "SiD letter of intent," Technical Report, preprint [arXiv:0911.0006](https://arxiv.org/abs/0911.0006) [physics.ins-det] (2009).

¹⁶T. Abe *et al.*, "The international large detector: Letter of intent," Technical Report, preprint [arXiv:1006.3396](https://arxiv.org/abs/1006.3396) [hep-ex] (2010).

¹⁷CLIC Conceptual Design Report, CERN-2012-007, Geneva, Switzerland, 2012.

¹⁸F. Simon, "Detector Systems at CLIC," *Physics Procedia* **37**, 63–71 (2012).

¹⁹C. Collette, S. Janssens, and D. Tshilumba, *Nucl. Instrum. Methods Phys. Res. A* **684**, 7–17 (2012).

²⁰A. Gaddi, H. Gerwig, N. Siegrist, and F. Ramos, "Dynamic analysis of the ff magnets pre-isolator and support system," Technical Report EDMS n1098581, 2010.

²¹F. Lackner, K. Artoos, C. Collette, H. Mainaud Durand, C. Hauviller, J. Kemppinen, and R. Leupe, "Development of an excentric cam based active pre-alignment system for the CLIC main beam quadrupole magnet," in *Proceedings of the 6th International Workshop on Mechanical Engineering Design of Synchrotron Radiation Equipment and Instrumentation (MEDSI00)* (Oxford, United Kingdom, 2010).

²²A. Preumont, J.-P. Dufour, and C. Malekian, *J. Guid. Control Dyn.* **15**, 390–395 (1992).

²³A. Preumont, *Vibration Control of Active Structures. An Introduction*, 3rd ed. (Kluwer Academic, Dordrecht, The Netherlands, 2011).

²⁴Y. Achkire, "Active tendon control of cable-stayed bridges," Ph.D. dissertation (University of Brussels, Belgium, 1997).

²⁵B. de Marneffe, "Active and passive vibration isolation and damping via shunted transducers," Ph.D. dissertation (University of Brussels, Belgium, 2007).